




Side-by-side comparison of the two widely studied GRPR radiotracers, radiolabeled NeoB and RM2, in a preclinical setting

T. S. T. Damiana¹ · P. Paraíso¹ · C. de Ridder² · D. Stuurman¹ · Y. Seimbille¹ · S. U. Dalm¹ 

Received: 28 April 2023 / Accepted: 24 July 2023
© The Author(s) 2023

Abstract

Introduction NeoB and RM2 are the most investigated gastrin-releasing peptide receptor (GRPR)-targeting radiotracers in preclinical and clinical studies. Therefore, an extensive side-by-side comparison of the two radiotracers is valuable to demonstrate whether one has advantages over the other. Accordingly, this study aims to compare the *in vitro* and *in vivo* characteristics of radiolabeled NeoB and RM2 to guide future clinical studies.

Method The stability of the radiolabeled GRPR analogs was determined in phosphate buffered saline (PBS), and commercially available mouse and human serum. Target affinity was determined by incubating human prostate cancer PC-3 cells with [¹⁷⁷Lu]Lu-NeoB or [¹⁷⁷Lu]Lu-RM2, +/– increasing concentrations of unlabeled NeoB, RM2, or Tyr⁴-bombesin (BBN). To determine uptake and specificity cells were incubated with [¹⁷⁷Lu]Lu-NeoB or [¹⁷⁷Lu]Lu-RM2 +/– Tyr⁴-BBN. Moreover, *in vivo* studies were performed to determine biodistribution and pharmacokinetics. Finally, radiotracer binding to various GRPR-expressing human cancer tissues was investigated.

Results Both radiotracers demonstrated high stability in PBS and human serum, but stability in mouse serum decreased substantially over time. Moreover, both radiotracers demonstrated high GRPR affinity and specificity, but a higher uptake of [¹⁷⁷Lu]Lu-NeoB was observed in *in vitro* studies. *In vivo*, no difference in tumor uptake was seen. The most prominent difference in uptake in physiological organs was observed in the GRPR-expressing pancreas; [¹⁷⁷Lu]Lu-RM2 had less pancreatic uptake and a shorter pancreatic half-life than [¹⁷⁷Lu]Lu-NeoB. Furthermore, [¹⁷⁷Lu]Lu-RM2 presented with a lower tumor-to-kidney ratio, while the tumor-to-blood ratio was lower for [¹⁷⁷Lu]Lu-NeoB. The autoradiography studies revealed higher binding of radiolabeled NeoB to all human tumor tissues.

Conclusion Based on these findings, we conclude that the *in vivo* tumor-targeting capability of radiolabeled NeoB and RM2 is similar. Additional studies are needed to determine whether the differences observed in physiological organ uptakes, i.e., the pancreas, kidneys, and blood, result in relevant differences in organ absorbed doses when the radiotracers are applied for therapeutic purposes.

Keywords GRPR · NeoB · RM2 · Peptide receptor radionuclide therapy · Prostate cancer

Introduction

The gastrin-releasing peptide receptor (GRPR) is a G protein-coupled receptor belonging to the family of bombesin (BBN) receptors. The receptor is expressed in the pancreas, and very low levels have also been reported in the colon, prostate, and some regions of the central nervous system.

Stimulation of GRPR can induce several pharmacological and biological responses, such as smooth muscle contraction and hormone secretion [1]. Next to the physiological expression, overexpression of GRPR has been reported in various cancer types, including lung-, breast- (BC), pancreatic-, prostate- (PCa), head and neck cancer, and neuroblastomas/glioblastomas [2–4]. Due to its overexpression in these cancer types, radiotracers targeting the GRPR have been developed for peptide receptor radionuclide imaging and therapy (PRRT) [5–7]. Both GRPR-targeted analogs with agonistic and antagonistic properties have been developed and evaluated. GRPR antagonists have shown superior tumor uptake and pharmacokinetic properties compared to agonists. Furthermore, the use of GRPR antagonists prevents adverse side effects, e.g., nausea and

✉ S. U. Dalm
s.dalm@erasmusmc.nl

¹ Department of Radiology & Nuclear Medicine, Erasmus Medical Center, Rotterdam, The Netherlands

² Department of Experimental Urology, Erasmus Medical Center, Rotterdam, The Netherlands

diarrhea, caused by receptor activation that was previously observed with agonists [8–10]. Radiolabeled GRPR antagonists studied during the past years include, e.g., RM1, RM2, SB3, NeoB, ProBOMB, and RM26, of which NeoB and RM2 are the two most investigated GRPR-targeting radiotracers in preclinical and clinical studies [11–16]. The structural difference between NeoB and RM2 can be found at the C-terminal sequence and the linker that connects the chelator to the targeting moiety (Fig. 1). The C-terminus of NeoB consists of (His¹²)-NH-CH[CH₂-CH(CH₃)₂], and the universal DOTA-chelator is connected to a *p*-aminomethylaniline-diglycolic acid (*p*ADA) linker at the N-terminus [14, 17, 18]. RM2 has a (His¹²)-Sta¹³-Leu¹⁴-NH₂ sequence at the C-terminus, and the N-terminal DOTA-chelator is conjugated to a 4-amino-1-carboxymethylpiperidine (Pip) linker [19].

Radiolabeled NeoB and RM2 have demonstrated promising results in preclinical and clinical studies [17, 18, 20, 21]. Currently, a phase I/IIa clinical trial (NeoRay, NCT03872778) is ongoing in which the safety, tolerability, pharmacokinetics, distribution, radiation dosimetry, and anti-tumor activity of [¹⁷⁷Lu]Lu-NeoB are investigated in patients with tumors known to overexpress GRPR. Another clinical trial is planning to investigate different doses of [¹⁷⁷Lu]Lu-NeoB in combination with radiotherapy and

temozolomide in newly diagnosed patients with glioblastoma (NCT05739942). Regarding RM2, two ongoing trials, i.e. NCT03113617 and NCT02624518, using gallium-68 labeled RM2 PET/CT and PET/MRI, respectively, are evaluating its potential to detect PCa.

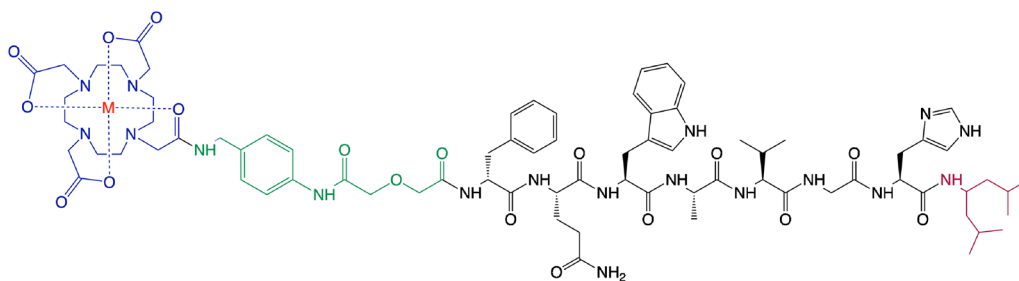
An extensive side-by-side comparison of the radiotracers can be valuable to demonstrate whether one has specific advantages over the other to guide future (clinical) studies. Therefore, the current study aims to accurately compare stability, target affinity, specificity, biodistribution, and pharmacokinetics of radiolabeled NeoB and RM2 to guide future clinical studies.

Material and methods

Chemistry and radiolabeling

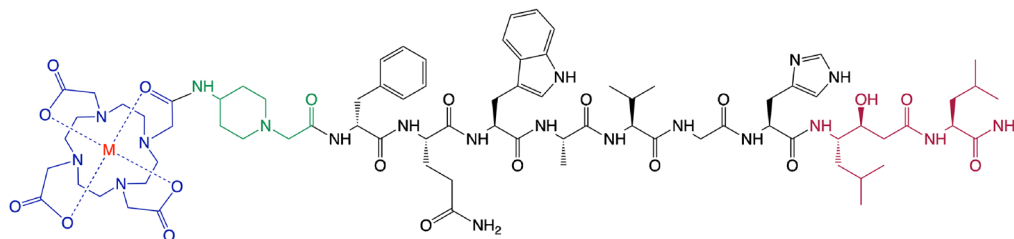
NeoB and RM2 were synthesized as described in Supplementary material 1. Both peptides were labeled with lutetium-177 (LuMark®, IDB Holland, The Netherlands) for all in vitro cell studies and in vivo studies. For autoradiography studies, the peptides were labeled with indium-111 (Covidien, The Netherlands) [22]. Lutetium-177 or indium-111 was added to NeoB and RM2, together with

NeoB



DOTA - *p*-aminomethylaniline-diglycolic acid (*p*ADA) - D-Phe - Gln - Trp - Ala - Val - Gly - His - NH-CH[CH₂-CH(CH₃)₂]₂

RM2



DOTA - 4-amino-1-carboxymethylpiperidine (Pip) - D-Phe - Gln - Trp - Ala - Val - Gly - His - Sta - Leu -NH₂

Fig. 1 Chemical structures of NeoB and RM2. Blue: chelator, green: linker, black (and red) targeting moiety (and c-terminus)

water (109 μL), sodium acetate (1 μL , 2.5 M, pH 4.5), ascorbic/gentisic acids (10 μL , 50 mM) and L-methionine (10 μL , 50 mM) to prevent radiolysis [23]. The mixtures were incubated at 90 °C for 20 min and then left to cool down for 5 min. For all in vitro assays and autoradiography studies, the peptides were labeled with a molar activity of 20 MBq/nmol. The in vivo studies were performed with a molar activity of 60 MBq/nmol. The radiolabeling yield (RCY) was determined by instant thin-layer chromatography on silica-gel-impregnated glass fiber sheets (Agilent, The Netherlands) eluted with a solution of sodium citrate (0.1 M, pH 5), in order to monitor the completion of the labeling reactions. Unbound lutetium-177 was complexed to diethylenetriaminepentaacetic acid (DTPA), which is known to be excreted immediately after in vivo injection in mice [24]. Furthermore, data was corrected for RCY by multiplying counts per minute with the determined correction factor (100%/RCY%). Additionally, Kolliphor HS 15 (2 mg/ml; Sigma Aldrich, USA) was added to all radiolabelings to prevent sticking of the peptides. The radiochemical purity (RCP) was determined by radio-high pressure liquid chromatography (HPLC) (LC/MS 1260 Infinity II system, Agilent, The Netherlands) (Supplementary material 1).

Stability studies in PBS, and mouse and human serum

The ^{177}Lu -labeled peptides were incubated in 300- μL phosphate buffered saline (PBS; Gibco, ThermoFisher, The Netherlands) at 37 °C, and their stability was verified after 1, 4, 24, 48, and 72 h by radio-HPLC (Supplementary Fig. 2). The stability in serum was determined by incubating the radiolabeled compounds into 300 μL of mouse serum (Invitrogen, USA) or human serum (Sigma Aldrich, USA) at 37 °C (Supplementary Fig. 3, 4). At each time point post-incubation, 35 μL of the mixture was added to an Eppendorf tube, and the proteins were precipitated by adding an equal volume of acetonitrile. The tubes were centrifuged at 16,000 rpm, 4 °C for 20 min, and the stability was monitored by radio-HPLC, expressed as the RCP at the different time points.

Cell culture

PC-3 cells were cultured in Ham's F-K12 nutrient mix (Gibco, ThermoFisher, The Netherlands) supplemented with 10% fetal bovine serum (Gibco, ThermoFisher, The Netherlands), penicillin (100 IU/ml, Gibco, ThermoFisher, The Netherlands) and streptomycin (100 $\mu\text{g}/\text{ml}$, Gibco, ThermoFisher, The Netherlands) at 37 °C in a humidified atmosphere of 5% CO_2 of air (NuAire).

Competition binding assay and uptake

PC-3 cells were seeded at 2.5×10^5 cells/well into 12 well plates 18–24 h prior to the experiment. Cells were incubated with 10^{-9} M of [^{177}Lu]Lu-NeoB or [^{177}Lu]Lu-RM2 together with increasing concentrations (10^{-12} – 10^{-6} M) of unlabeled NeoB, RM2, or Tyr⁴-bombesin (BBN; Sigma Aldrich, The Netherlands) (an analogue of natural occurring bombesin, thus an agonist) for 1 h at 37 °C. Hereafter, cells were washed twice with PBS and subsequently lysed with 0.1 M NaOH for 20 min at room temperature (RT). The cell lysates were collected and measured using a gamma counter (1480 WIZARD automatic γ -counter, PerkinElmer, The Netherlands). For the uptake studies, PC-3 cells (2.5×10^5) were incubated with 10^{-9} M of [^{177}Lu]Lu-NeoB or [^{177}Lu]Lu-RM2 with or without 10^{-6} M Tyr⁴-BBN for 1 h at 37 °C. Hereafter, cells were washed twice with cold PBS and lysed with 0.1 M NaOH for 20 min at RT. The cell lysates were collected and measured to determine the amount of radioactivity in a gamma counter. To correct for cell density, cells from two separate wells were counted (Countess counter, Invitrogen, The Netherlands), and data was expressed as percentage of added dose (AD) per 2.5×10^5 cells.

Animal model

All animal experiments were approved by the Animal Welfare Committee of the Erasmus MC, and all experiments were conducted in accordance to institutional guidelines. Male NMRI-Foxn1 nu/nu mice (5 weeks old) were subcutaneously inoculated with 5×10^6 PC-3 cells on the right shoulder (100 μL : 1/3 Matrigel (Corning, The Netherlands) and 2/3 Hank's Balanced Salt Solution (Gibco, ThermoFisher, The Netherlands). Tumors were grown for 3 weeks resulting in an average volume of $362 \pm 102 \text{ mm}^3$.

In vivo biodistribution

PC-3 tumor-bearing mice were intravenously injected with 200 μL of 9 MBq/150 pmol [^{177}Lu]Lu-NeoB or [^{177}Lu]Lu-RM2. At 1, 4, 24, 48, and 72 h post-injection (p.i.), animals were sedated using 2.5% isoflurane in oxygen, and blood was collected via the orbital vein, after which the animals were euthanized using cervical dislocation. Subsequently, the following organs were collected; the tail, tumor, spleen, liver, pancreas, small intestine, colon, coecum, kidneys, lung, and muscle. To assess in vivo specificity of [^{177}Lu]Lu-NeoB and [^{177}Lu]Lu-RM2, an additional group of tumor-bearing animals was injected with the radiolabeled peptides plus an 196-fold excess of Tyr⁴-BBN and biodistribution studies were performed as described above at 4 h p.i. The collected tumor and organs were weighed, and the radioactivity was measured in the gamma counter.

The biodistribution data are expressed as percentage injected dose per gram of tissue (% ID/g). Animal numbers per group are indicated in Supplementary Table 1 and 2.

SPECT/CT imaging

Whole-body single-photon emission computed tomography and computed tomography (SPECT/CT; VECTor/CT, MILabs, The Netherlands) were acquired in PC-3 tumor-bearing mice 1, 4, and 24 h p.i. of 9 MBq/150 pmol of [^{177}Lu]Lu-NeoB or [^{177}Lu]Lu-RM2 under sedation (2.5% isoflurane in oxygen) with body temperature maintained by a heating pad ($N=1$ per radiotracer and per time point). The CT was obtained using the following parameters: 50 kV, 210 μA , 2 bed positions, and an acquisition time of 5 min. SPECT scans were acquired with the XXUHS-M, 3 mm collimator in list mode using 35 bed positions with an acquisition time of 30 min. Images were reconstructed using MILabs rec 12 using the SROSEM method with the following parameters: voxel size 0.4 mm; 9 iterations and 128 subsets; and 1 mm FWHM Gaussian filter. Post-analysis of the scans were performed using the Imalytics preclinical software (Gremse-IT, Germany). After each scan, animals were euthanized, and the organs were collected for biodistribution purposes, as described above.

Autoradiography on human tumor and healthy tissue

Fresh frozen tissues of 3 human prostate cancers (PCa), breast cancers (BC), and gastrointestinal stromal tumors (GIST) were sectioned into 10- μm thick slices and mounted onto glass slides (ThermoFisher, The Netherlands). The tissue slices were pre-incubated with washing buffer (167 mM Tris-HCL (pH 7.6), 5 mM MgCl_2) containing 0.25% BSA for 10 min at RT. Hereafter, tissue slides were incubated with 10^{-9} M of [^{111}In]In-NeoB or [^{111}In]In-RM2 with or without 10^{-6} M Tyr⁴-BBN for 1 h at RT. Following incubation, slides were washed 3 times, dried, and loaded into the BeaQuant (Atlantic Instruments for Research, France) for 48 h, and analyzed using Beamage software (Atlantic Instruments for Research, France). Quantified binding to tumor tissue was corrected for unspecific binding (quantified signal from blocked tissues). To allow comparison of separate experiments, the background signal was also quantified and subtracted. The data are expressed as % AD/ mm^2/min .

Statistics

Statistical analysis was performed using Graphpad Prism version 9.0.0. Outliers were identified using the ROUT method with a Q value of 1%. IC₅₀ curves were determined using non-linear regression. Significant differences

between the IC₅₀ and uptake values of radiolabeled NeoB and RM2 were determined using an unpaired t test. The tumor half-life of [^{177}Lu]Lu-NeoB was determined using a non-linear regression followed by an uptake and excretion curve. To determine the tumor half-life of [^{177}Lu]Lu-RM2 and the pancreas half-lives of both radiotracers a non-linear regression was applied followed by a one phase decay model. Significant differences between the tumor/organ uptake and tumor/organ half-lives of radiolabeled NeoB and RM2 derived from the biodistribution studies were determined using a 2-way ANOVA.

Results

Stability

[^{177}Lu]Lu-NeoB and [^{177}Lu]Lu-RM2 were obtained in > 98% RCY and > 97% RCP. Both radiotracers showed excellent stability in PBS up to 24 h at 37 °C (Table 1, Supplementary Fig. 2). However, after 48 h, [^{177}Lu]Lu-RM2 stability in PBS slightly decreased in a time dependent manner while that of [^{177}Lu]Lu-NeoB was maintained. Stability studies in mouse serum showed a decrease in stability over time for both [^{177}Lu]Lu-NeoB ($94.3 \pm 0.7\%$ intact radiotracer at 1 h vs. $4.4 \pm 1.2\%$ at 72 h) and [^{177}Lu]Lu-RM2 ($90.9 \pm 0.5\%$ intact radiotracer at 1 h vs. $5.3 \pm 0.9\%$ at 72 h) (Table 1, Supplementary Fig. 3). The stability of both [^{177}Lu]Lu-NeoB and [^{177}Lu]Lu-RM2 in human serum was noticeably superior to their stability in mouse serum (Table 1, Supplementary Fig. 4). [^{177}Lu]Lu-NeoB stability in human serum, however, was slightly higher at the 1 and 4 h time point, and slightly lower at the 24, 48, and 72 h time point.

In vitro competition binding and uptake

The competition binding assay was performed to determine the affinity of ^{177}Lu -labeled NeoB and RM2. The concentration of unlabeled NeoB, RM2, and Tyr⁴-BBN needed to block 50% of ^{177}Lu -labeled NeoB or RM2, were all in the nanomolar (nM) range (Fig. 2). However, more unlabeled NeoB, RM2 and Tyr⁴-BBN were required to block 50% of [^{177}Lu]Lu-NeoB compared to the amount needed to block 50% of [^{177}Lu]Lu-RM2 uptake (Table 2).

This was also reflected in the uptake of the radiotracers; the uptake of [^{177}Lu]Lu-NeoB was $21.90 \pm 3.76\%$ AD, while this was $10.96 \pm 3.46\%$ AD for [^{177}Lu]Lu-RM2 (Fig. 2c). For both [^{177}Lu]Lu-NeoB and [^{177}Lu]Lu-RM2, the uptake in the presence of Tyr⁴-BBN was low (< 1% AD), demonstrating specificity of binding.

Table 1 Stability in PBS, mouse and human serum of [¹⁷⁷Lu]Lu-NeoB and [¹⁷⁷Lu]Lu-RM2, (N=3)*

	[¹⁷⁷ Lu]Lu-NeoB					[¹⁷⁷ Lu]Lu-RM2						
	0 h	1 h	4 h	24 h	48 h	72 h	0 h	1 h	4 h	24 h	48 h	72 h
PBS (%)	97.1 ± 0.3	97.8 ± 0.3	97.4 ± 0.5	96.3 ± 0.3	95.1 ± 0.4	93.8 ± 0.9	97.4 ± 0.3	97.8 ± 0.4	96.7 ± 0.5	95.6 ± 0.3	87.6 ± 0.6	80.4 ± 0.8
Mouse serum (%)		94.3 ± 0.7	84.1 ± 1.1	27.9 ± 2.3	14.2 ± 1.0	4.4 ± 1.2		90.9 ± 0.5	73.6 ± 0.4	29.6 ± 1.2	17.1 ± 3.5	5.3 ± 0.9
Human serum (%)		97.9 ± 0.2	97.8 ± 0.3	89.2 ± 0.5	81.0 ± 0.7	75.6 ± 1.7		96.7 ± 0.7	95.5 ± 1.1	94.9 ± 1.5	92.3 ± 1.9	88.4 ± 0.6

*Results are expressed as mean percentage ± SD of intact radiolabeled ligand (RCP) after incubation at 37 °C of three experiments

Biodistribution

Biodistribution studies were performed at 1, 4, 24, 48, and 72 h p.i. of [¹⁷⁷Lu]Lu-NeoB or [¹⁷⁷Lu]Lu-RM2 (Fig. 3A and B, Supplementary table 1 and 2). No significant differences were observed in tumor uptake of [¹⁷⁷Lu]Lu-NeoB and [¹⁷⁷Lu]Lu-RM2 at any time point. However, a difference in uptake in background organs was observed between the radiotracers, resulting in a difference in tumor-to-organ ratios. At all investigated time points, animals injected with [¹⁷⁷Lu]Lu-NeoB had a lower tumor-to-blood, tumor-to-liver, tumor-to-pancreas, and tumor-to-gastrointestinal tract ratio, but a higher tumor-to-kidney ratio compared to animals that received [¹⁷⁷Lu]Lu-RM2 (Fig. 3c and d). Among all collected organs, the GRPR-expressing pancreas showed the highest radiotracer uptake with both [¹⁷⁷Lu]Lu-NeoB and [¹⁷⁷Lu]Lu-RM2 at the 1 h time point, resulting in the lowest tumor-to-organ ratio for this organ. However, pancreatic uptake was significantly higher with [¹⁷⁷Lu]Lu-NeoB compared to [¹⁷⁷Lu]Lu-RM2. At the 1 h time point, the tumor and pancreatic uptake of [¹⁷⁷Lu]Lu-NeoB was 9.38 ± 0.81% ID/g and 30.66 ± 4.29% ID/g, respectively, while for [¹⁷⁷Lu]Lu-RM2 this was 9.27 ± 1.81% ID/g and 14.39 ± 2.56% ID/g, respectively (Supplementary table 1 and 2). The pancreas remained the organ with the highest uptake over time in animals that received [¹⁷⁷Lu]Lu-NeoB, but this was not the case for animals that received [¹⁷⁷Lu]Lu-RM2; the kidneys were the organ with the highest uptake from 24 p.i. onwards with [¹⁷⁷Lu]Lu-RM2. Therefore, the tumor-to-pancreas ratios remained the most unfavorable for [¹⁷⁷Lu]Lu-NeoB, but for [¹⁷⁷Lu]Lu-RM2 the tumor-to-kidney ratio was lowest of all tumor-to-organ ratios at the 24, 48, and 72 h time points (Fig. 3c and d).

Blocking studies 4 h p.i. reduced tumor and pancreatic uptake of both radiotracers, but did not block uptake completely. For [¹⁷⁷Lu]Lu-NeoB tumor uptake was 9.98 ± 2.64% ID/g vs. 4.55 ± 0.42% ID/g when Tyr⁴-BBN was co-injected, and pancreatic uptake was 21.35 ± 3.05% ID/g vs. 14.48 ± 2.40% ID/g, respectively. For [¹⁷⁷Lu]Lu-RM2, this was 9.14 ± 0.94% ID/g vs. 3.27 ± 0.46% ID/g for the tumor, and 2.07 ± 0.30% ID/g vs. 0.49 ± 0.08% ID/g for the pancreas.

SPECT/CT images acquired at 1, 4, and 24 h p.i. of [¹⁷⁷Lu]Lu-NeoB or [¹⁷⁷Lu]Lu-RM2 were in line with the biodistribution data (Fig. 4). Due to the high uptake of both [¹⁷⁷Lu]Lu-NeoB or [¹⁷⁷Lu]Lu-RM2, the tumor could be visualized already at 1 h p.i. The only physiological organs visible at this time point were the pancreas, kidneys, and the bladder.

Clearance

Despite the high pancreatic uptake of the radiotracers, clearance was fast. However, the pancreatic half-life of [¹⁷⁷Lu]Lu-NeoB was significantly higher compared to that of RM2;

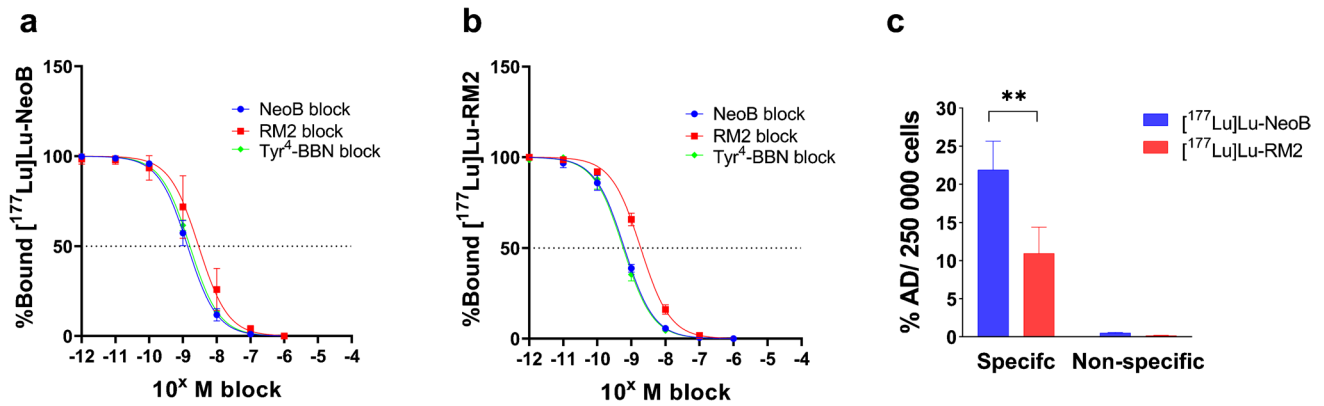


Fig. 2 Binding of **a** [^{177}Lu]Lu-NeoB and **b** [^{177}Lu]Lu-RM2 in the presence of increasing concentrations of unlabeled NeoB, RM2, or Tyr⁴-BBN. **c** Specific (total) uptake shown for [^{177}Lu]Lu-NeoB and

[^{177}Lu]Lu-RM2. Non-specific uptake was determined in the presence of a 1000 times excess of Tyr⁴-BBN. Data are shown as mean %AD/250 000 cells \pm SD. * $P \leq 0.05$; ** $P \leq 0.01$; *** $P \leq 0.001$

7.19 ± 2.09 h vs. 1.07 ± 0.29 h ($P < 0.001$), respectively. The tumor half-life was 41.29 ± 12.98 h for [^{177}Lu]Lu-NeoB and 51.22 ± 15.17 h for [^{177}Lu]Lu-RM2 (Fig. 5).

Autoradiography

The autoradiography studies revealed a higher binding of [^{111}In]In-NeoB to PCa, BC, and GIST tissues (Fig. 6). Tyr⁴-BBN did not completely block [^{111}In]In-NeoB and [^{111}In]In-RM2 in the BC tissues, while this was the case for PCa and GIST tissues.

Discussion and conclusion

Several GRPR analogs have been and are being developed for targeted radionuclide imaging and PRRT of GRPR-expressing tumors. In order to guide future studies, we compared the two most studied GRPR-targeting radiolabeled antagonists, NeoB and RM2. Overall, the stability of both radiotracers in PBS and human serum was high. The stability in mouse serum, however, decreased relatively fast over time. As both [^{177}Lu]Lu-NeoB and [^{177}Lu]Lu-RM2 are peptide-based molecules, which are known for their fast pharmacokinetics, it seems unlikely that the low percentage of intact radiotracer after 24 h impacts our results.

Table 2 IC₅₀ values for unlabeled NeoB, RM2, and Tyr⁴-BBN as mean \pm SD

	[^{177}Lu]Lu-NeoB	[^{177}Lu]Lu-RM2	<i>P</i> value
NeoB block	1.42 ± 0.41 nM	0.63 ± 0.04 nM	0.01
RM2 block	3.53 ± 2.36 nM	1.90 ± 0.31 nM	0.3
Tyr ⁴ -BBN block	1.61 ± 0.18 nM	0.58 ± 0.05 nM	<0.001

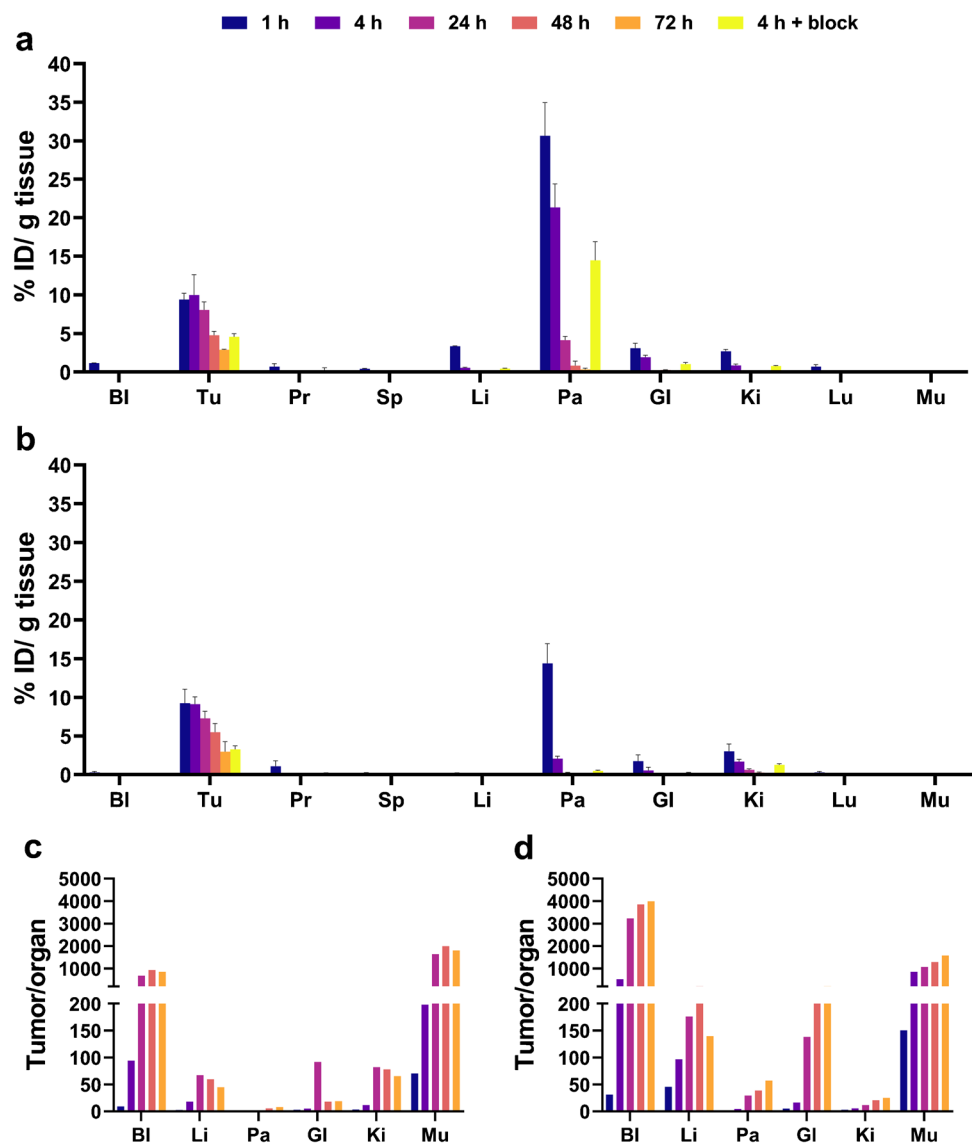
N = At least 3

In a recent study, Gunther et al. [25] also compared the stability of the two radiotracers. The authors reported [^{177}Lu]Lu-NeoB to be more stable than [^{177}Lu]Lu-RM2 in both human and mouse plasma. The differences observed in stability reported by Gunther et al. and the current study are most likely due to differences in the experimental setup. First, we used quenchers which have previously shown to prevent radiolysis [23]. Secondly, in the study by Gunther et al., radiotracer stability was determined in plasma, while we performed our stability studies in serum. Finally, in the previously published study, the stability in mouse plasma was determined in vivo (30 min p.i.), while in the current study the radiolabeled tracers were incubated in commercially available human and mouse serum in vitro.

We also demonstrated that both radiolabeled GRPR analogs bind with good affinity to their target. However, NeoB showed a slightly better GRPR affinity and accordingly radiolabeled NeoB had a higher uptake than radiolabeled RM2 in vitro, which is in accordance with the study by Gunther et al. [25]. Furthermore, our autoradiography study revealed higher binding of radiolabeled NeoB in all investigated human cancer samples. For this study, we have selected 3 cancer types which are known to have high GRPR expression [26]. In our PCa samples, however, we observed low binding of both radiotracers. Although PCa is commonly associated with high(er) GRPR expression, this may vary significantly depending on, among other factors, the disease stage. Nevertheless, we were able to demonstrate differences in binding of radiolabeled NeoB and RM2 on these cancer tissues.

The in vitro cell and tissue models provide information about the affinity and binding capabilities of the radiotracers, but do not take their pharmacokinetic properties into account. We have therefore included extensive biodistribution and imaging studies. The results showed that the more favorable GRPR affinity and higher uptake/binding of radiolabeled NeoB observed in vitro did not translate to

Fig. 3 Biodistribution profile of **a** [^{177}Lu]Lu-NeoB and **b** [^{177}Lu]Lu-RM2 at 1, 4, 24, 48, 72 h p.i. of PC-3 tumor-bearing mice. Tumor to background ratio of organs of interest calculated from the biodistribution data of **c** [^{177}Lu]Lu-NeoB and **d** [^{177}Lu]Lu-RM2. BI= blood; Tu=PC-3 tumor; Pr= prostate; Sp= spleen; Li= liver; Pa= pancreas; GI= gastrointestinal tract; Ki= kidney; Lu= lungs; Mu= muscle



higher tumor uptake of the radiotracer in vivo; [^{177}Lu]Lu-NeoB and [^{177}Lu]Lu-RM2 had similar tumor uptake values in vivo at all investigated time points. The difference in in vitro and in vivo uptake is most likely caused by the difference of the radiotracer pharmacokinetics in the two systems. Furthermore, the significantly higher pancreatic uptake of [^{177}Lu]Lu-NeoB compared to [^{177}Lu]Lu-RM2 might have led to lower [^{177}Lu]Lu-NeoB tumor uptake than expected based on the in vitro findings.

During the in vitro cell studies, Tyr⁴-BBN successfully displaced [^{177}Lu]Lu-NeoB and [^{177}Lu]Lu-RM2 from GRPR binding sites on PC-3 cells, indicating specificity, but the molecule was less effective in blocking GRPR-mediated uptake of both radiotracers in vivo. Other studies reported similar findings when blocking with Tyr⁴-BBN in vivo [13, 14]. Tyr⁴-BBN is an agonist which triggers internalization of the receptor-ligand complex upon binding and potentially

also recycling of the receptor back to the membrane hereafter. If the GRPR becomes available at the membrane again, the antagonistic radiotracers can again bind to the receptor [27, 28]. This can occur both in vitro and in vivo, but during our in vitro studies cells were incubated for only 1 h with the radiotracers while the in vivo block studies were performed 4 h p.i. of the radiotracers. The latter might be enough time for the proposed mechanism to occur. Future studies should use antagonists for blocking purposes. Regarding Tyr⁴-BBN, to confirm our hypothesis, studies should be performed at early and extended incubation periods.

In the autoradiography studies, Tyr⁴-BBN was also unable to completely block binding of the radiotracers to BC tissues. The high density of connective tissue present in these samples might have led to unspecific binding of the peptides to the tissues. NeoB, based on its structure and partition coefficient (LogD), is more lipophilic than RM2

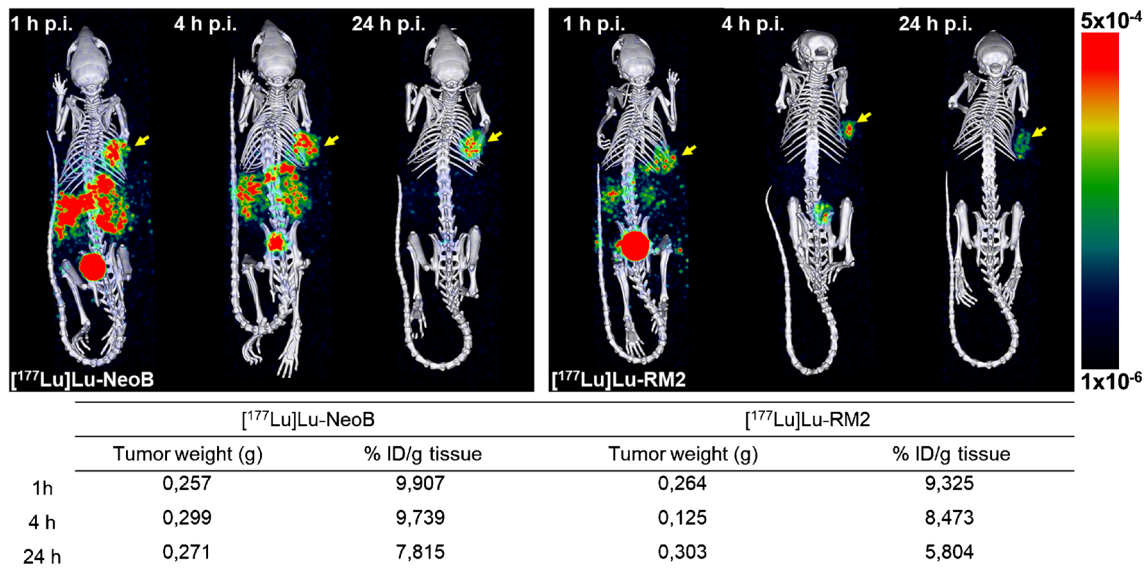


Fig. 4 SPECT/CT images of PC-3 tumor-bearing mice 1, 4, and 24 h p.i. of (left) $[^{177}\text{Lu}]\text{Lu-NeoB}$ and (right) $[^{177}\text{Lu}]\text{Lu-RM2}$. The tumor is located on the right shoulder and is indicated with a yellow arrow. $N=1$

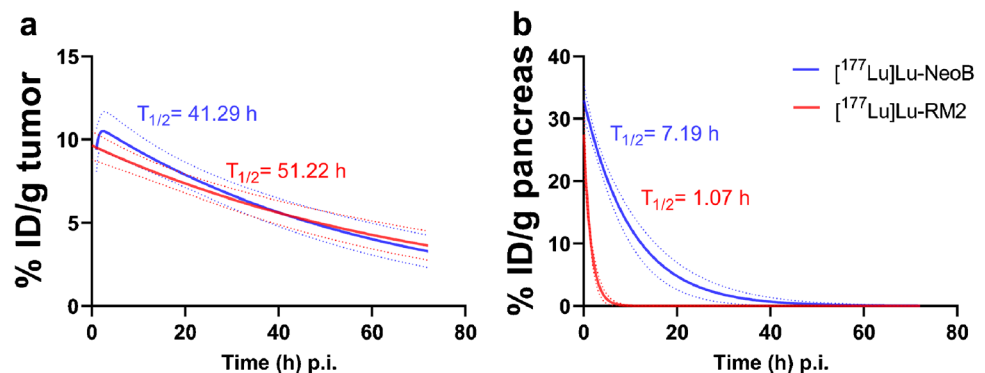
[25, 29], which might have led to a higher unspecific binding of this radiotracer. In our autoradiography studies we corrected the quantified values for un-specific binding and thus the aforementioned does not influence the analysis with respect to comparison of binding of the two radiotracers to the evaluated human cancers.

In the biodistribution study, besides tumor and pancreatic uptake, low uptake in the liver, kidney, and gastrointestinal tract was observed with both $[^{177}\text{Lu}]\text{Lu-NeoB}$ and $[^{177}\text{Lu}]\text{Lu-RM2}$. The tumor-to-liver ratio observed with $[^{177}\text{Lu}]\text{Lu-NeoB}$ was lower compared to that of $[^{177}\text{Lu}]\text{Lu-RM2}$. Liver uptake of radiolabeled NeoB has also been reported by others and suggests hepatic clearance of the compound [30]. The radiolabeled NeoB molecules that are cleared hepatically might be those that were initially taken up by the pancreas. After being metabolized in the pancreas, they are carried to the liver via the hepatic portal vein for excretion [31, 32]. The lower pancreatic uptake and the faster pancreatic

clearance of $[^{177}\text{Lu}]\text{Lu-RM2}$ might explain why lower liver uptake was observed for $[^{177}\text{Lu}]\text{Lu-RM2}$. Additionally, the observed liver uptake might also be linked to the lipophilicity of the compounds, as lipophilic compounds tend to have higher liver uptake.

Regarding the pancreatic uptake, the off target uptake in this organ is important when it comes to potential radiotoxicity during/after PRRT. The difference that was observed in pancreatic uptake between $[^{177}\text{Lu}]\text{Lu-NeoB}$ and $[^{177}\text{Lu}]\text{Lu-RM2}$, resulting in a more favorable tumor-to-pancreas ratio for $[^{177}\text{Lu}]\text{Lu-RM2}$, can potentially be explained by a difference in affinity for the murine GRPR between the two radiotracers. In an attempt to elucidate the above, we performed autoradiography studies on mouse and human pancreas tissue. However, only slight binding was observed to the mouse pancreas tissue, and no binding was observed to human pancreas tissue (data for mouse pancreas shown in Supplementary Fig. 5). This is most likely because the

Fig. 5 Pharmacokinetic modeling of the **a** tumor and **b** pancreas half-life clearance for $[^{177}\text{Lu}]\text{Lu-NeoB}$ and $[^{177}\text{Lu}]\text{Lu-RM2}$



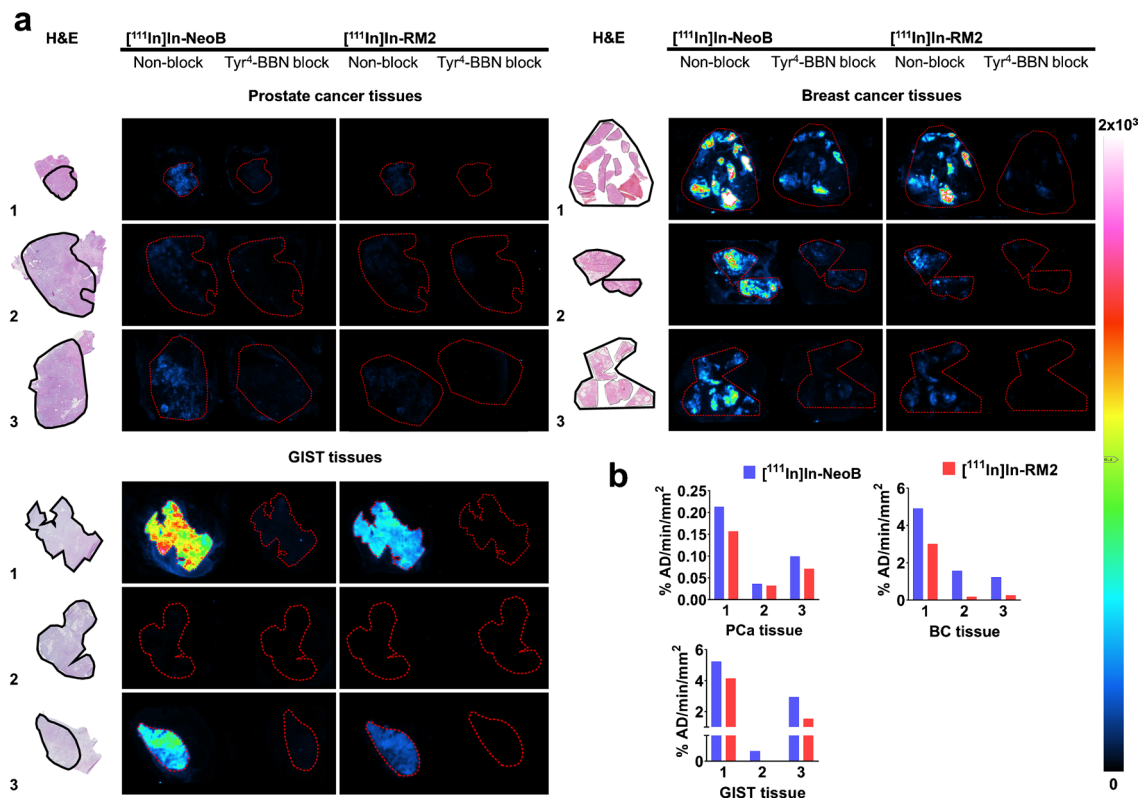


Fig. 6 a In vitro autoradiography of $[^{111}\text{In}]\text{In-NeoB}$ and $[^{111}\text{In}]\text{In-RM2}$ performed on GRPR-expressing human PCa, BC, GIST tumor tissues. Samples are from different patients. **b** % AD/min/mm²

calculated for the region of interests for marked on the H&E (black line) and the ARG (red dotted line) samples. Artefact hotspots were removed from the $[^{111}\text{In}]\text{In-NeoB}$ blocked PCa tissue 3

receptor was only present at low density or not present at all on the cells of the mouse and human pancreas, respectively; at the moment, the analysis was performed. As the organ is full of enzymes, the GRPR is most likely degraded enzymatically during tissue collection and storage. In addition to the difference in affinity for the mouse and human GRPR, factors such as microvasculature and perfusion [33] can also cause a discrepancy in results obtained in mice vs. men.

Moreover, whether or not the pancreas is at risk and should be considered as a dose-limiting organ in GRPR-mediated PRRT has been investigated by several groups. Even though we did not study the toxicity of the radiotracers in the current study, the pancreatic half-life of the radiotracers observed suggests that the dose to which the organ is exposed is limited. Furthermore, in a recently published clinical study by Kurth et al., it was reported that $[^{177}\text{Lu}]\text{Lu-RM2}$ was well tolerated by all patients [20]. The authors reported that $[^{177}\text{Lu}]\text{Lu-RM2}$ showed high uptake in the tumor and cleared rapidly from normal organs, including the pancreas. Regarding NeoB, a pre-clinical study has shown $[^{177}\text{Lu}]\text{Lu-NeoB}$ to be well tolerated after repeated radiotracer administration. In the above-mentioned study, radiotoxic effects were found in the kidneys [30]. In our study, a more unfavorable tumor-to-kidney ratio was observed with

$[^{177}\text{Lu}]\text{Lu-RM2}$ compared to $[^{177}\text{Lu}]\text{Lu-NeoB}$; however, the kidney uptake was only significantly higher for $[^{177}\text{Lu}]\text{Lu-RM2}$ at the 4 h time point. Extensive dosimetry studies should be performed to demonstrate whether or not the dose to which the kidneys is exposed is relevantly higher with $[^{177}\text{Lu}]\text{Lu-RM2}$ vs. $[^{177}\text{Lu}]\text{Lu-NeoB}$.

In addition, a lower tumor-to-blood ratio was observed for $[^{177}\text{Lu}]\text{Lu-NeoB}$ vs. $[^{177}\text{Lu}]\text{Lu-RM2}$, indicating a faster clearance of $[^{177}\text{Lu}]\text{Lu-RM2}$ from the blood. As next to the kidneys, bone marrow is often a dose-limiting organ, extensive dosimetry studies should also be performed to determine whether this difference observed between the radiotracers is relevant. Of note, only at the earliest time points (1 h and 4 h), when radiotracer uptake was relatively high in the blood, differences in blood uptake was significant between the radiotracers. It should also be mentioned that in the previously mentioned preclinical study evaluating $[^{177}\text{Lu}]\text{Lu-NeoB}$ toxicity, no lasting hematological effects were observed after treatment [30]. The tumor-to-organ ratios, except the tumor-to-kidney ratios observed between $[^{177}\text{Lu}]\text{Lu-NeoB}$ and $[^{177}\text{Lu}]\text{Lu-RM2}$ in this study, showed similar patterns as those calculated in the study of Gunther et al. [25]. However, in the study of Gunther et al., the tumor-to-kidney ratio for $[^{177}\text{Lu}]\text{Lu-NeoB}$ and $[^{177}\text{Lu}]\text{Lu-RM2}$ were

similar. This discrepancy might be a consequence of differences in experimental setup (e.g., labeling, injected dose, mouse strain) between our study and theirs. Strategies to decrease physiologic uptake in the background organs and increase tumor uptake are being evaluated by various groups. Wang et al., developed a series of GRPR antagonists (TacsBOMB1-5) based on the following sequence [Leu¹³ψThz¹⁴] Bombesin(7–14) of which TacsBOMB5 demonstrated significantly higher PC-3 tumor uptake and lower pancreatic uptake than RM2 [34]. It should be noted that this study was performed in a mouse models and might be different in humans, e.g., a difference in affinity for the murine and human GRPR might be at play. Another promising approach to reduce pancreatic uptake involves bioorthogonal chemistry, also known as the pretargeting strategy. Compared to conventional targeted therapies, pretargeting leads to higher tumor/background ratios, reduced circulation time of radioactivity, and facilitates the use of short-lived radionuclides [35–37]. D’Onofrio et al. developed a GRPR pretargeting radiocomplex which has successfully reduced pancreatic uptake [36]. However, uptake in the tumor was also diminished due to rapid washout and fast metabolism of the compound *in vivo*. Currently, pretargeting radiocomplexes with higher stability and longer circulation time are being developed.

To our knowledge, there is no head-to-head comparison of radiolabeled NeoB and RM2 in patients and comparing results of separately performed studies is challenging due to methodological differences and differences in the patient’s characteristics. Despite this, we attempted to compare dosimetry calculations reported in two clinical studies using [⁶⁸Ga]Ga-NeoB and [⁶⁸Ga]Ga-RM2 [38, 39]. In this comparison, the reported dose delivered to the pancreas, liver, and bladder was higher with radiolabeled NeoB vs. radiolabeled RM2. Furthermore, the analysis revealed no difference in kidney uptake between radiolabeled NeoB and RM2. The findings of this indirect comparison are in line with our study, with regards to a higher pancreatic and liver uptake with radiolabeled NeoB compared to radiolabeled RM2, and partly also for the kidney uptake as previously mentioned we only observed a significant difference in kidney uptake at the 4 h time point. However, a direct clinical comparison of the radiotracers is necessary to confirm these findings. Furthermore, the above findings might suggest that if a difference in affinity for the murine and human GRPR between the two radiotracers exists, this only partly explains our *in vivo* findings as also in humans’ radiolabeled NeoB results in a higher pancreatic dose.

To summarize, our studies demonstrated good stability of the two GRPR radiotracers up to 24 h, and specific and high uptake of the radiotracers *in vitro* and *in vivo*. Regarding the latter, uptake/binding was higher for radiolabeled NeoB *in vitro* on PC-3 cells and human cancer tissues, but

no differences in tumor uptake was observed *in vivo* in PC-3 xenografts. Both radiotracers showed pancreatic uptake, but this was significantly lower for [¹⁷⁷Lu]Lu-RM2. Additionally, the pancreas half-life was faster for this radiotracer. Moreover, a lower tumor-to-blood ratio was observed for [¹⁷⁷Lu]Lu-NeoB, while tumor-to-kidney was lower for [¹⁷⁷Lu]Lu-RM2. Based on these findings, we conclude that the *in vivo* tumor targeting capability of radiolabeled NeoB and RM2 are similar. However, patient studies should confirm whether the differences in uptake in background organs (e.g., pancreas, liver, kidney, blood) and pharmacokinetics are similar in humans, as this can be an important factor to consider when applying the radiotracers for PRRT.

Supplementary Information The online version contains supplementary material available at <https://doi.org/10.1007/s00259-023-06364-4>.

Acknowledgements The authors thank A.L. Van den Berg for assisting with the *in vitro* work and Dr. C.H.M. van Deurzen for histopathological analysis of the tumor tissue.

Funding This work was partly supported by NWO ZonMw Veni #09150161810061.

Data Availability The datasets generated during the current study are available from the corresponding author on reasonable request.

Declarations

Ethics approval All animal experiments were approved by the Animal Welfare Committee of the Erasmus MC, and all experiments were conducted in accordance to institutional guidelines.

Competing interest SD receives financial support from Advanced Accelerator Applications, a Novartis Company, for an unrelated project.

Open Access This article is licensed under a Creative Commons Attribution 4.0 International License, which permits use, sharing, adaptation, distribution and reproduction in any medium or format, as long as you give appropriate credit to the original author(s) and the source, provide a link to the Creative Commons licence, and indicate if changes were made. The images or other third party material in this article are included in the article's Creative Commons licence, unless indicated otherwise in a credit line to the material. If material is not included in the article's Creative Commons licence and your intended use is not permitted by statutory regulation or exceeds the permitted use, you will need to obtain permission directly from the copyright holder. To view a copy of this licence, visit <http://creativecommons.org/licenses/by/4.0/>.

References

- Jensen RT, et al. International Union of Pharmacology. LXVIII. Mammalian bombesin receptors: nomenclature, distribution, pharmacology, signaling, and functions in normal and disease states. *Pharmacol Rev.* 2008;60(1):1–42.
- Gonzalez N, et al. Bombesin-related peptides and their receptors: recent advances in their role in physiology and disease states. *Curr Opin Endocrinol Diabetes Obes.* 2008;15(1):58–64.

3. Patel O, Shulkes A, Baldwin GS. Gastrin-releasing peptide and cancer. *Biochim Biophys Acta*. 2006;1766(1):23–41.
4. Ischia J, et al. Expression and function of gastrin-releasing peptide (GRP) in normal and cancerous urological tissues. *BJU Int*. 2014;113(Suppl 2):40–7.
5. Li X, et al. New frontiers in molecular imaging using peptide-based radiopharmaceuticals for prostate cancer. *Front Chem*. 2020;8: 583309.
6. Schroeder RP, et al. A standardised study to compare prostate cancer targeting efficacy of five radiolabelled bombesin analogues. *Eur J Nucl Med Mol Imaging*. 2010;37(7):1386–96.
7. Mansi R et al. Radiolabeled bombesin analogs. *Cancers (Basel)*. 2021;13(22):5766.
8. Baratto L, Jadvar H, Iagaru A. Prostate cancer theranostics targeting gastrin-releasing peptide receptors. *Mol Imaging Biol*. 2018;20(4):501–9.
9. Maina T, Nock BA. From bench to bed: new gastrin-releasing peptide receptor-directed radioligands and their use in prostate cancer. *PET Clin*. 2017;12(2):205–17.
10. Maina T, et al. Theranostic prospects of gastrin-releasing peptide receptor-radioantagonists in oncology. *PET Clin*. 2017;12(3):297–309.
11. Sah BR, et al. Dosimetry and first clinical evaluation of the new 18F-radiolabeled bombesin analogue BAY 864367 in patients with prostate cancer. *J Nucl Med*. 2015;56(3):372–8.
12. Bratanovic IJ, et al. A radiotracer for molecular imaging and therapy of gastrin-releasing peptide receptor-positive prostate cancer. *J Nucl Med*. 2022;63(3):424–30.
13. Maina T, et al. Preclinical and first clinical experience with the gastrin-releasing peptide receptor-antagonist [(6)(8)Ga]SB3 and PET/CT. *Eur J Nucl Med Mol Imaging*. 2016;43(5):964–73.
14. Nock BA, et al. Theranostic perspectives in prostate cancer with the gastrin-releasing peptide receptor antagonist NeoBOMB1: preclinical and first clinical results. *J Nucl Med*. 2017;58(1):75–80.
15. Wieser G, et al. Diagnosis of recurrent prostate cancer with PET/CT imaging using the gastrin-releasing peptide receptor antagonist (68)Ga-RM2: preliminary results in patients with negative or inconclusive [(18)F]Fluoroethylcholine-PET/CT. *Eur J Nucl Med Mol Imaging*. 2017;44(9):1463–72.
16. Zhang J, et al. PET using a GRPR antagonist (68)Ga-RM26 in healthy volunteers and prostate cancer patients. *J Nucl Med*. 2018;59(6):922–8.
17. Dalm SU, et al. 68Ga/177Lu-NeoBOMB1, a novel radiolabeled GRPR antagonist for theranostic use in oncology. *J Nucl Med*. 2017;58(2):293–9.
18. Kaloudi A et al. NeoBOMB1, a GRPR-antagonist for breast cancer theragnostics: first results of a preclinical study with [(67)Ga]NeoBOMB1 in T-47D cells and tumor-bearing mice. *Molecules*. 2017;22(11):1950.
19. Mansi R, et al. Development of a potent DOTA-conjugated bombesin antagonist for targeting GRPr-positive tumours. *Eur J Nucl Med Mol Imaging*. 2011;38(1):97–107.
20. Kurth J, et al. First-in-human dosimetry of gastrin-releasing peptide receptor antagonist [(177)Lu]Lu-RM2: a radiopharmaceutical for the treatment of metastatic castration-resistant prostate cancer. *Eur J Nucl Med Mol Imaging*. 2020;47(1):123–35.
21. Iagaru A. Will GRPR compete with PSMA as a target in prostate cancer? *J Nucl Med*. 2017;58(12):1883–4.
22. Schroeder RP, et al. Improving radiopeptide pharmacokinetics by adjusting experimental conditions for bombesin receptor-targeted imaging of prostate cancer. *Q J Nucl Med Mol Imaging*. 2012;56(5):468–75.
23. de Blois E, et al. Effectiveness of quenchers to reduce radiolysis of (111)In- or (177)Lu-labelled methionine-containing regulatory peptides. Maintaining radiochemical purity as measured by HPLC. *Curr Top Med Chem*. 2012;12(23):2677–85.
24. Breeman WA, et al. The addition of DTPA to [177Lu-DOTA0, Tyr3]octreotate prior to administration reduces rat skeleton uptake of radioactivity. *Eur J Nucl Med Mol Imaging*. 2003;30(2):312–5.
25. Gunther T, et al. Substitution of L-tryptophan by alpha-methyl-L-tryptophan in (177)Lu-RM2 results in (177)Lu-AMTG, a high-affinity gastrin-releasing peptide receptor ligand with improved in vivo stability. *J Nucl Med*. 2022;63(9):1364–70.
26. Cornelio DB, Roesler R, Schwartzmann G. Gastrin-releasing peptide receptor as a molecular target in experimental anticancer therapy. *Ann Oncol*. 2007;18(9):1457–66.
27. Yuan L, et al. 14-3-3 signal adaptor and scaffold proteins mediate GPCR trafficking. *Sci Rep*. 2019;9(1):11156.
28. Brandenburg LO, Pufe T, Koch T. Role of phospholipase d in g protein coupled receptor function. *Membranes (Basel)*. 2014;4(3):302–18.
29. Tsopelas F, Giaginis C, Tsantili-Kakoulidou A. Lipophilicity and biomimetic properties to support drug discovery. *Expert Opin Drug Discov*. 2017;12(9):885–96.
30. Ruigrok EAM, et al. Safety of [(177)Lu]Lu-NeoB treatment: a preclinical study characterizing absorbed dose and acute, early, and late organ toxicity. *Eur J Nucl Med Mol Imaging*. 2022;49(13):4440–51.
31. Harkins JM, Ahmad B. Anatomy, Abdomen and Pelvis, Portal Venous System (Hepatic Portal System) [Updated 2022 Aug 8]. In: StatPearls [Internet]. Treasure Island (FL): StatPearls Publishing; 2023. Available from: <https://www.ncbi.nlm.nih.gov/books/NBK554589/>
32. Carneiro C, et al. All about portal vein: a pictorial display to anatomy, variants and physiopathology. *Insights Imaging*. 2019;10(1):38.
33. Dolensek J, Rupnik MS, Stozer A. Structural similarities and differences between the human and the mouse pancreas. *Islets*. 2015;7(1): e1024405.
34. Wang L et al. (68)Ga-labeled [Leu(13)psiThz(14)]Bombesin(7–14) derivatives: promising GRPR-targeting PET tracers with low pancreas uptake. *Molecules*. 2022;27(12):3777.
35. Handula M, Chen KT, Seimbille Y. IEDDA: an attractive bioorthogonal reaction for biomedical applications. *Molecules*. 2021;26(15):4640.
36. D’Onofrio A et al. Bioorthogonal chemistry approach for the theranostics of GRPR-expressing cancers. *Pharmaceutics*. 2022;14(12):2569.
37. Verhoeven M, Seimbille Y, Dalm SU. Therapeutic applications of pretargeting. *Pharmaceutics*. 2019;11(9):434.
38. Haendeler M, et al. Biodistribution and radiation dosimetric analysis of [68Ga]Ga-RM2: a potent GRPR antagonist in prostate carcinoma patients. *Radiation*. 2021;1(1):33–44.
39. Gruber L, et al. MITIGATE-NeoBOMB1, a phase I/IIa study to evaluate safety, pharmacokinetics, and preliminary imaging of (68)Ga-NeoBOMB1, a gastrin-releasing peptide receptor antagonist. *GIST patients J Nucl Med*. 2020;61(12):1749–55.

Publisher's note Springer Nature remains neutral with regard to jurisdictional claims in published maps and institutional affiliations.